IEEE Photonics Journal
An IEEE Photonics Society Publication

Open Access

Dual-Wavelength Spectroscopy of a Metallic-Grating-Coupled Surface Plasmon Resonance Biosensor

Volume 7, Number 2, April 2015

Farshid Bahrami
J. Stewart Aitchison, Member, IEEE
Mo Mojahedi, Member, IEEE

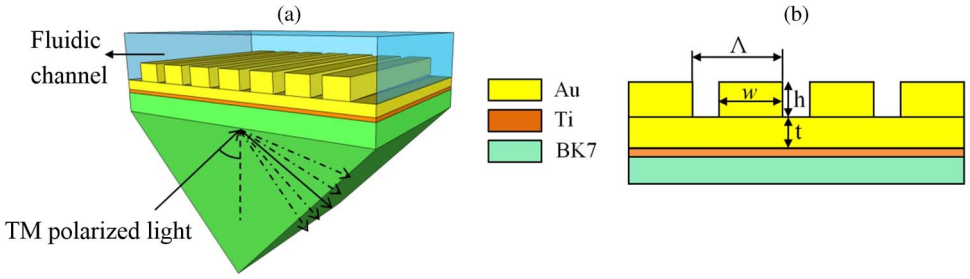

DOI: 10.1109/JPHOT.2015.2416335
1943-0655 © 2015 IEEE

IEEE photonics SOCIETY

IEEE

Dual-Wavelength Spectroscopy of a Metallic-Grating-Coupled Surface Plasmon Resonance Biosensor

Farshid Bahrami, J. Stewart Aitchison, *Member, IEEE*, and Mo Mojahedi, *Member, IEEE*

Department of Electrical Engineering, Faculty of Applied Science and Engineering, University of Toronto, Toronto, ON M5S 3G4 Canada

DOI: 10.1109/JPHOT.2015.2416335

Manuscript received February 22, 2015; revised March 13, 2015; accepted March 19, 2015. Date of current version April 14, 2015. This work was supported by the Natural Science and Engineering Research Council of Canada—BiopSys Network under Grant 486537. Corresponding author: F. Bahrami (e-mail: farshid.bahrami@mail.utoronto.ca).

Abstract: A novel approach is proposed to decouple the surface and bulk effects in surface plasmon resonance (SPR) biosensors. This method is based on a metallic-grating-based SPR in which a sensor is efficiently optimized to excite three surface plasmon waves at two different wavelengths. Decoupling surface and bulk effects can be realized using this technique by tracing the resonance angle variations corresponding to each excited mode. To optimize the sensor, a genetic algorithm is applied, and finally, the performance of the sensor is compared with the conventional single-interface SPR biosensor.

Index Terms: Plasmonics, gratings, sensors, spectroscopy, biosensors.

1. Introduction

For several decades, surface plasmon resonance sensors have become a leading technology in the field of biosensors, mainly due to their high sensitivity. However their performance suffers from one of their main inherent limitations called sensitivity to interfering effects [1]. This limitation is due to the fact that surface plasmon resonance (SPR) mode extends beyond the adlayer (bio-molecular layer to be detected) and interacts with the fluid (bulk) above the metal surface. Any variations in the properties of the adlayer (thickness and index) or the bulk fluid index (n_b) can affect the propagation constant of the SPR wave and, hence, the output signal. Therefore, single SPR spectroscopy cannot differentiate between refractive index changes in the bulk fluid and the binding-induced refractive index changes at the sensing surface.

The most common method to remove the interfering effects is to increase the number of independent measurements. Multi-channel SPR sensors have been implemented to increase the number of simultaneous measurements by adding a reference channel beside the sensing channel [2]. Although decoupling the surface effects from the bulk index variations is achievable through this approach, decoupling adlayer thickness (d_a) and index (n_a) from the output signal is still not possible. In addition, to cancel out the interfering effects, an ideal reference channel should be exactly identical to the sensing channel in all aspects, with the exception of the one measurand being measured. This is a requirement which is not easy to meet in practice.

Several methods have been proposed to extract two different parameters from the output signal (e.g., the refractive index and thickness of the adlayer). These methods can be summarized into six categories: I) measurements at two different fluid indices [3], II) angular spectroscopy at two different wavelengths [4], III) wavelength spectroscopy at two different angles [5], IV) multi-mode SPR spectroscopy [6], V) dual polarization spectroscopy [7], and VI) SPR spectrum analysis using a multilayer Fresnel theory [8].

Three-plasmon spectroscopy is one possible method to extract all the interfering effects (n_a, d_a, n_b) from the output signal. In this regard, Homola *et al.* [9], have proposed a new approach to deconvolve the aforementioned interfering effects. This technique is based on measurements at three different wavelengths using wavelength modulation. Since this platform requires direct excitation of a multi-diffractive grating through a flow cell with transparent top, the interaction between the external light and the fluid materials can create errors in measurement.

We have recently reported a new approach to overcome the cross sensitivity to the interfering surface and bulk effects using a dielectric grating based SPR sensor [10] which enables three-mode spectroscopy at two different polarizations. In this work, a novel approach for SPR biosensing using a metallic grating based SPR sensor (MGSPR) is proposed. This approach benefits from one of the unique features of the grating, which is splitting the incoming light into several diffraction orders, for SPR sensing in Kretschmann configuration. The rigorous coupled-wave analysis (RCWA) method is applied to study the effect of the grating on the performance of the sensor. A metallic grating is optimized so that three SPR waves at two different wavelengths are excited. Thus, the adlayer properties (d_a and n_a) can be determined and differentiated from the bulk index (n_b) variations by dual wavelength measurements. Finally, the optimum design along with a method to decouple the interfering effects is presented.

2. Metallic Grating Based SPR Sensor

One of the most common techniques to excite the SPR wave in biosensing is the Kretschmann configuration [11]. In this method, a prism with higher index of refraction than the top dielectric layer is used to excite the surface plasmon wave. The dispersion relation between the incident light frequency (ω) and the surface plasmon wavevector (K_{SPR}) is shown as

$$K_{\mathrm{SPR}} = \frac{\omega}{c}\sqrt{\frac{\varepsilon_m \varepsilon_S}{\varepsilon_m + \varepsilon_S}} = k_0 n_p \sin(\theta_{\mathrm{SPR}}) \tag{1}$$

where θ_{SPR}, ε_m, ε_s, ω, c, n_p, and k_0 represent the angle of incident at the resonance, metal permittivity, solution permittivity, incident light angular frequency, speed of light, prism index of refraction, and the incident light wavevector.

In order to improve the performance of the SPR based biosensors, metallic gratings have been widely used [12]. The main use of the metallic grating in prism based SPR sensors is improving the sensitivity by creating local field enhancement and increasing sensing surface area [13]. Assuming that the dispersion properties of SPR wave is not disturbed by the grating, the momentum conservation between the free space light and the SPR wave in MGSPR sensor can be expressed as [14]

$$\pm\sqrt{\frac{\varepsilon_m \varepsilon_S}{\varepsilon_m + \varepsilon_S}} = n_p \sin(\theta_{\mathrm{SPR}}) + m\frac{\lambda}{\Lambda} \tag{2}$$

where m, λ, and Λ represent the diffraction orders, incident light wavelength and the period of the grating. In (2), the incident light wavevector is distorted by the grating which generates series of diffracted beams directed away from the corrugated surface [see Fig. 1(a)]. Sign "+" and sign "−" in (2) correspond to positive $(m > 0)$ and negative $(m < 0)$ diffracted orders. The diffraction orders (m) which satisfy (2) can excite SPR wave and create a resonance dip in the reflectance spectrum. In this work, the possibility of SPR spectroscopy at a fixed wavelength with more than one diffracted order is investigated. Fig. 1(b) shows a 2-D cross section view of the MGSPR sensor along with the grating parameters.

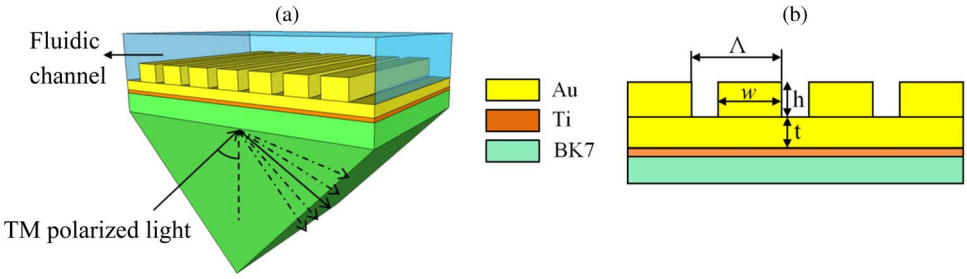

Fig. 1. (a) Three-dimensional schematic of a MGSPR sensor. (b) 2-D cross section of the MGSPR sensor. Gold nanowires of a rectangular profile are assumed to be infinite in length with periodicity of Λ, thickness of h and a filling factor of w/Λ.

3. Numerical Model

One of the most common tools to study periodic nanostructures is the RCWA which is an exact solution of Maxwell's equations for electromagnetic diffraction by grating and is well explained by Moharam *et al.* [15]. In order to improve the convergence rate especially for the TM polarization, an efficient implementation of RCWA is applied [16].

To simultaneously excite multiple SPR waves in a prism-grating based geometry, several parameters should be adjusted which are listed here: grating periodicity, grating height, filling factor, gold thickness, and incident wavelength. Any variations in the aforementioned parameters can alter the propagation constant of the mode. The optimization of these parameters should be so that each of the excited modes show high sensitivity to the surface or bulk effects. Therefore defining a proper figure of merit (FoM) is necessary to evaluate the mode's characteristics.

Finding a suitable FoM is essential to make a qualitative analysis on the sensing performance of each mode. In most practical affinity biosensors the minimum detectible amount of the quantity to be measured, called *limit of detection* (LoD), is of interest. The LoD is inversely proportional to the product of sensor's sensitivity also called sensitivity factor (SF) and sensor merit (SM)—which is the ratio of the resonance depth over the full width at half maximum (FWHM). The product of SF and SM is called the combined sensitivity factor $(\text{CSF} = \text{SF} \times \text{SM})$. The exact definitions of SF and SM for bulk and surface sensing are explained in details in our previous work [17]. In this work, FoM is defined as the superposition of CSF corresponding to each mode

$$\text{FoM} = \sum_i \text{CSF}_i, \qquad i = 1, 2, \ldots \tag{3}$$

To optimize the proposed biosensor, the genetic algorithm (GA) is considered among other optimization techniques. GA is a promising optimization tool, especially when several design parameters should be optimized simultaneously.

4. Results and Discussion

Due to the computational intensity of the problem, distributed-memory parallelization is employed for design optimization. The computations herein were performed on the General Purpose Cluster at the University of Toronto Scinet supercomputer. The MGSPR is first optimized to excite two modes each highly sensitive to the surface effects. To have a qualitative comparison, single interface SPR sensor is also optimized with a GA. In the optimization process, BK7 glass is considered as the substrate and prism material in both structures and 2 nm Ti adhesion layer on the glass substrate is included in the simulation. Table 1 summarizes the optimized dimensions and wavelengths for both structures.

The reflected wave diffraction efficiency of the optimized MGSPR at 845 nm wavelength is shown in Fig. 2(a). There are two resonances in this spectrum corresponding to two

TABLE 1
Optimized dimensions of SPR and MGSPR sensors for affinity sensing

	Wavelength (nm)	Gold thickness (t)	Grating thickness(h)	Periodicity (Λ)	Fill factor (w/ Λ)
SPR	915	50nm	–	–	–
MGSPR	845	26nm	241nm	325nm	0.7

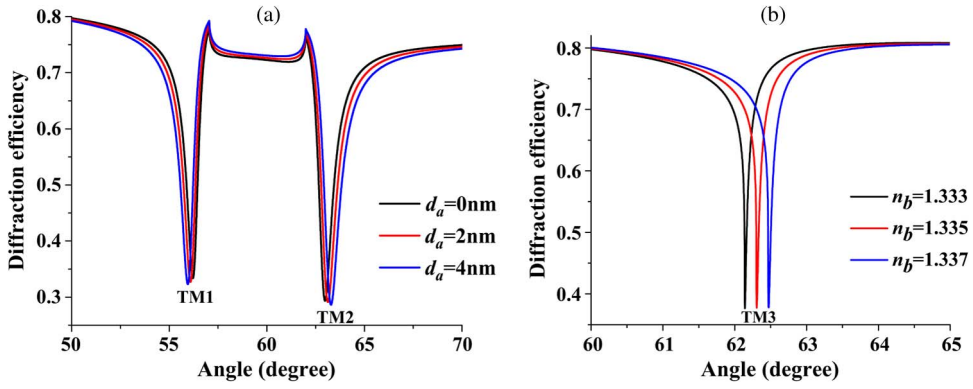

Fig. 2. Diffraction efficiency of the reflected light with TM polarization for the optimized MGSPR sensor at the incident wavelength of (a) 845 nm ($n_{BK7} = 1.51$, $n_{Au} = 0.19 + 5.54i$, $n_{Ti} = 3.04 + 3.31i$, and $n_{water} = 1.329$) and (b) 970 nm ($n_{BK7} = 1.51$, $n_{Au} = 0.24 + 6.6i$, $n_{Ti} = 3.3 + 3.26i$, and $n_{water} = 1.327$). d_a is the adlayer thickness and n_b is the bulk refractive index.

counter-propagating plasmonic modes with different propagation constants. These modes are highly sensitive to the surface parameters (n_a, d_a).

The first mode (TM1) with smaller angle of resonance is excited by the first negative diffraction order $(m = -1)$ and the second mode (TM2) with larger resonance angle is excited by the zeroth diffraction order $(m = 0)$. Both modes are excited efficiently which can be realized by the small values of the diffraction efficiency at the resonance angles in Fig. 2(a).

As mentioned earlier, the main goal of this work is to determine three interfering effects by three-mode spectroscopy. Two of the modes are excited at 845 nm wavelength and the third mode (TM3) can be generated by using a second wavelength (970 nm) optimized for high sensitivity to the bulk refractive index variations [see Fig. 2(b)]. This mode (TM3) is also excited by the zeroth diffraction order of the MGSPR sensor.

To further investigate the properties of the excited modes, dispersion curves can be used. An indirect method to extract the dispersion relation is to calculate the reflection or transmission spectrum for a range of incident angles and wavelengths. In this paper, RCWA is used to calculate the dispersion curve of the MGSPR sensor by finding the reflected light diffraction efficiency for a range of wavelengths as is shown in Fig. 3(a). Fig. 3(b) shows a dispersion curve which is analytically derived from (2). The two dominants reflectance minimums in Fig. 3(a) are originated by the same diffracted orders shown in Fig. 3(b). The small mismatch between these two dispersion curves is hidden in the fact that the dispersion equation is derived based on the assumption that the single interface SPR wave propagation constant is not disturbed by the presence of the grating.

The performance characteristics of each mode to the variations in surface and bulk parameters are shown in Table 2 in which the calculated values of the CSF with respect to the adlayer thickness (CSF_{thick}), adlayer index (CSF_{index}), and the bulk index (CSF_{bulk}) for both MGSPR and SPR sensors are summarized.

The optimized SPR sensor has large values of CSF for both the surface and bulk effects. This causes more cross-sensitivity to the interfering surface and bulk effects which is not

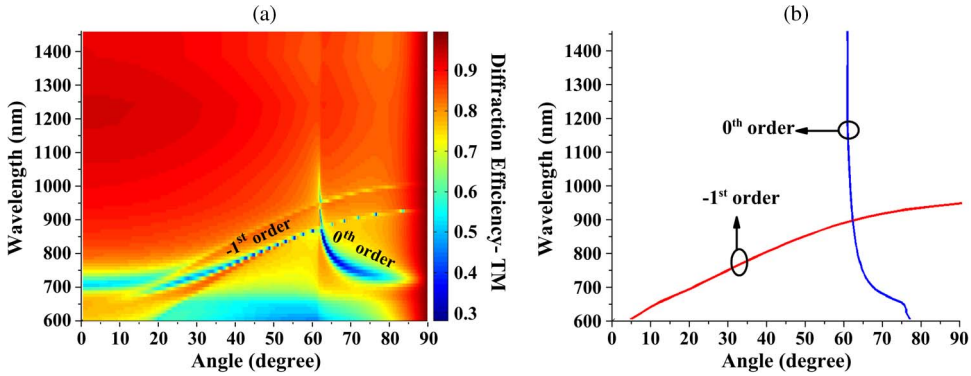

Fig. 3. (a) Dispersion relation of the MGSPR sensor calculating using RCWA. (b) Analytically calculated dispersion relation of the SPR wave in the optimized MGSPR sensor using (2).

TABLE 2

Optimized performance characteristics for single interface SPR and MGSPR sensors

Sensor	First Mode (TM1)			Second Mode (TM2)			Third Mode (TM3)		
	CSF_{thick} (nm^{-1})	CSF_{index} (RIU^{-1})	CSF_{bulk} (RIU^{-1})	CSF_{thick} (nm^{-1})	CSF_{index} (RIU^{-1})	CSF_{bulk} (RIU^{-1})	CSF_{thick} (nm^{-1})	CSF_{index} (RIU^{-1})	CSF_{bulk} (RIU^{-1})
SPR	0.05	0.7	96	–	–	–	–	–	–
MGSPR	0.04	0.6	42	0.04	0.54	44	0.02	0.29	369

possible to decouple with single mode spectroscopy. However, the MGSPR sensor has two modes (TM1, TM2) each highly sensitive to the surface effects and a third mode (TM3) with large sensitivity to the bulk effect. Therefore, by measuring the variations of the resonance angles at two different wavelengths in the MGSPR sensor, determining two surface and one bulk effects is possible.

In order to extract the variation in surface and bulk effects from multimode spectroscopy, we assume that the resonance angles of the modes are linearly related to the changes in the solution refractive index and to the properties of adlayer [18]. Therefore, the variations in the interfering effects can be expressed as

$$\begin{pmatrix} \Delta d_a \\ \Delta n_a \\ \Delta n_b \end{pmatrix} = S^{-1} \times \begin{pmatrix} \Delta\theta_{M1}(\lambda_1) \\ \Delta\theta_{M2}(\lambda_1) \\ \Delta\theta_{M3}(\lambda_2) \end{pmatrix}, \quad S = \begin{pmatrix} \frac{\partial\theta_{M1}(\lambda_1)}{\partial d_a} & \frac{\partial\theta_{M1}(\lambda_1)}{\partial n_a} & \frac{\partial\theta_{M1}(\lambda_1)}{\partial nb} \\ \frac{\partial\theta_{M2}(\lambda_1)}{\partial d_a} & \frac{\partial\theta_{M2}(\lambda_1)}{\partial n_a} & \frac{\partial\theta_{M2}(\lambda_1)}{\partial nb} \\ \frac{\partial\theta_{M3}(\lambda_2)}{\partial d_a} & \frac{\partial\theta_{M3}(\lambda_2)}{\partial n_a} & \frac{\partial\theta_{M3}(\lambda_2)}{\partial n_b} \end{pmatrix} \tag{4}$$

where Δd_a, Δn_a, and Δn_b are the variations in adlayer thickness, adlayer refractive index and bulk refractive index, respectively. The S matrix contains the sensitivity of each mode to the interfering surface or bulk effects. The parameters which can be measured from the experiment are the resonance angle shifts and the bulk and surface sensitivities (S matrix). Equation (4) can be solved for Δd_a, Δn_a, and Δn_b only if S is not singular. The calculated S matrix corresponding to the MGSPR structure shown in Table 1 is presented as

$$S = \begin{pmatrix} 0.065 & 1.026 & 71.84 \\ 0.075 & 1.066 & 86.85 \\ 0.005 & 0.057 & 82.89 \end{pmatrix} \rightarrow |S| = 0.56. \tag{5}$$

The determinant value confirms that the S matrix is not singular.

To estimate how much the solutions of (4) can change in proportion to small changes in the input argument (shifts in resonance angle), a condition number for the S matrix should be calculated. Before calculating the condition number, each elements of the S matrix should be normalized to a typical value of its quantity to make the elements dimensionless. The calculated condition number for the S matrix is 44 which corresponds to one digit of maximum inaccuracy on top of what would be lost in the numerical method. This small condition number confirms that the S matrix is a well-conditioned matrix and the interfering effects can be calculated with enough accuracy. Therefore dual wavelength measurement with MGSPR sensor enables us to decouple the interfering surface $(\Delta d_a, \Delta n_a)$ and bulk (Δn_b) effects from the output signals.

5. Conclusion

A novel approach to solve one of the major shortcomings of the SPR biosensors which is sensitivity to the interfering surface and bulk effects was investigated. The proposed solution was based on three-mode spectroscopy using metallic grating based SPR platform. For this purpose, two diffracted waves of a metallic grating were utilized to excite two surface plasmon waves each with high affinity to surface effects. The second wavelength was optimized in order to excite a third mode with high sensitivity to the bulk fluid index variations. Finally, it was shown that determining the variations in adlayer thickness, adlayer index, and bulk fluid index is possible with enough accuracy. Therefore improving the biosensor functionality by extracting more information from the sensor is the key advantage of this approach.

Acknowledgment

The author would like to acknowledge the use of computing resources from West Grid.

References

[1] J. Homola, "Present and future of surface plasmon resonance biosensors," *Anal. Bioanal. Chem.*, vol. 377, no. 3, pp. 528–539, Oct. 2003.
[2] J. Homola, H. B. Lu, and S. S. Yee, "Dual-channel surface plasmon resonance sensor with spectral discrimination of sensing channels using dielectric overlayer," *Electron. Lett.*, vol. 35, no. 13, pp. 1105–1106, Jun. 1999.
[3] H. E. de Bruijn, B. S. F. Altenburg, R. P. H. Kooyman, and J. Greve, "Determination of thickness and dielectric constant of thin transparent dielectric layers using surface plasmon resonance," *Opt. Commun.*, vol. 82, no. 5/6, pp. 425–432, May 1991.
[4] K. A. Peterlinz and R. Georgiadis, "Two-color approach for determination of thickness and dielectric constant of thin films using surface plasmon resonance spectroscopy," *Opt. Commun.*, vol. 130, no. 4–6, pp. 260–266, Oct. 1996.
[5] K. S. Johnston, S. R. Karlsen, C. C. Jung, and S. S. Yee, "New analytical technique for characterization of thin films using surface plasmon resonance," *Mater. Chem. Phys.*, vol. 42, no. 4, pp. 242–246, Dec. 1995.
[6] S. Nizamov and V. M. Mirsky, "Self-referencing SPR-biosensors based on penetration difference of evanescent waves," *Biosens. Bioelectron.*, vol. 28, no. 1, pp. 263–269, Oct. 2011.
[7] F. Bahrami, M. Maisonneuve, M. Meunier, J. S. Aitchison, and M. Mojahedi, "Self-referenced spectroscopy using plasmon waveguide resonance biosensor," *Biomed. Opt. Exp.*, vol. 5, no. 8, pp. 2481–2487, Aug. 2014.
[8] J. M. Phelps and D. M. Taylor, "Determining the relative permittivity and thickness of a lossless dielectric overlayer on a metal film using optically excited surface plasmon polaritons," *J. Phys. D, Appl. Phys.*, vol. 29, no. 4, pp. 1080–1087, Apr. 1996.
[9] P. Adam, J. Dostálek, and J. Homola, "Multiple surface plasmon spectroscopy for study of biomolecular systems," *Sens. Actuators B, Chem.*, vol. 113, no. 2, pp. 774–781, Feb. 2006.
[10] F. Bahrami, J. S. Aitchison, and M. Mojahedi, "Multimode spectroscopy using dielectric grating coupled to a surface plasmon resonance sensor," *Opt. Lett.*, vol. 39, no. 13, pp. 3946–3949, Jul. 2014.
[11] J. Homola, S. S. Yee, and G. Gauglitz, "Surface plasmon resonance sensors: Review," *Sens. Actuators B, Chem.*, vol. 54, no. 1/2, pp. 3–15, Jan. 1999.
[12] S. Roh, T. Chung, and B. Lee, "Overview of plasmonic sensors and their design methods," in *Proc. Adv. Sensor Syst. Appl. IV*, 2010, p. 785 303.
[13] K. M. Byun, S. M. Jang, S. J. Kim, and D. Kim, "Effect of target localization on the sensitivity of a localized surface plasmon resonance biosensor based on subwavelength metallic nanostructures," *J. Opt. Soc. Amer. A, Opt. Image Sci. Vis.*, vol. 26, no. 4, pp. 1027–1034, Apr. 2009.
[14] J. Homola, I. Koudela, and S. S. Yee, "Surface plasmon resonance sensors based on diffraction gratings and prism couplers: Sensitivity comparison," *Sens. Actuators B, Chem.*, vol. 54, no. 1/2, pp. 16–24, Jan. 1999.

[15] M. G. Moharam, D. A. Pommet, E. B. Grann, and T. K. Gaylord, "Stable implementation of the rigorous coupled-wave analysis for surface-relief gratings: Enhanced transmittance matrix approach," *J. Opt. Soc. Amer. A, Opt. Image Sci. Vis.*, vol. 12, pp. 1077–1086, 1995.
[16] G. Granet and B. Guizal, "Efficient implementation of the coupled-wave method for metallic lamellar gratings in TM polarization," *J. Opt. Soc. Amer. A, Opt. Image Sci. Vis.*, vol. 13, no. 5, pp. 1019–1023, May 1996.
[17] F. Bahrami, M. Z. Alam, J. S. Aitchison, and M. Mojahedi, "Dual polarization measurements in the hybrid plasmonic biosensors," *Plasmonics*, vol. 8, no. 2, pp. 465–473, Jun. 2013.
[18] W. Lukosz and K. Tiefenthaler, "Sensitivity of integrated optical grating and prism couplers as (bio)chemical sensors," *Sens. Actuators*, vol. 15, no. 3, pp. 273–284, Nov. 1988.